AD-A266 957

‖‖‖‖‖‖‖‖‖‖‖‖

TECHNICAL REPORT NO. 2

Self-Diffusion Coefficients of Sol-Gel Intermediates

by

L. Ng and A.V. McCormick
Dept. of Chemical Engineering & Materials Science
University of Minnesota
421 Washington Ave. SE
Minneapolis, MN 55455

July 12, 1993

DTIC
S ELECTE D
JUL 19 1993
B

93 7 16 148

93-16242

‖‖‖‖‖‖‖‖‖‖

REPORT DOCUMENTATION PAGE

1. AGENCY USE ONLY (Leave blank)	2. REPORT DATE 7/12/93	3. REPORT TYPE AND DATES COVERED Technical

4. TITLE AND SUBTITLE	5. FUNDING NUMBERS
Self-Diffusion Coefficeinets of Sol-Gel Intermediates	N/N00014-91-J-1893

6. AUTHOR(S)
L. Ng, and A.V. McCormick

7. PERFORMING ORGANIZATION NAME(S) AND ADDRESS(ES)	8. PERFORMING ORGANIZATION REPORT NUMBER
Dept. of Chemical Engineering & Materials Science University of Minnesota 421 Washington Ave., SE Minneapolis, MN 55455	

9. SPONSORING/MONITORING AGENCY NAME(S) AND ADDRESS(ES)	10. SPONSORING/MONITORING AGENCY REPORT NUMBER
Office of Naval Research 800 N. Quincy Street Arlington, VA 22217	

11. SUPPLEMENTARY NOTES
submitted to AIChE J.

12a. DISTRIBUTION/AVAILABILITY STATEMENT	12b. DISTRIBUTION CODE
Reproduction in whole or in part is permitted for any purpose of the U.S. Government. This document has been approved for public release and sale; its distribution is unlimited.	

13. ABSTRACT (Maximum 200 words)

Over the past few decades, the sol-gel technique has shown great potential for producing ceramic materials of designed composition and properties. A typical sol-gel process involves the hydrolysis and polymerization of one or more metal alkoxides in an alcohol solution in a batch reactor to form a homogeneous gel, which is then further treated to provide the type of ceramic desired (aerogel, glass, crystal, coating, etc.).

Several authors have suggested that diffusion effects may influence the development of the gel microstructure. To investigate if diffusion effects are important, we begin by determining what governs the diffusivity of the precursors using the pulsed-gradient-spin-echo NMR technique. This report focuses on the early stages of the batch reaction.

The system chosen is the acid catalyzed hydrolysis and condensation of tetraethyl orthosilicate (TEOS) in ethanol. Our resultys from ^1H PGSE NMR and ^{29}Si NMR show that the diffusivities of the silicate precursors are not just a function of the molecular weight. Hydrogen bonding between the polar functional groups and the solvent also decreases the mobility of the reactants. Moreover, since hydrolysis

14. SUBJECT TERMS	15. NUMBER OF PAGES
Diffusion, ^{29}Si NMR, pulsed field gradient ^1H NMR sol/gel	21
	16. PRICE CODE

17. SECURITY CLASSIFICATION OF REPORT	18. SECURITY CLASSIFICATION OF THIS PAGE	19. SECURITY CLASSIFICATION OF ABSTRACT	20. LIMITATION OF ABSTRACT
unclassified	unclassified	unclassified	UL

Preprint: for   AIChE J.

Self-Diffusion Coefficients of Sol-Gel Intermediates

L. V. Ng and A. V. McCormick*, Chemical Engineering and Materials Science Department, University of Minnesota, Minneapolis, MN 55455.

ABSTRACT

Over the past few decades, the sol-gel technique has shown great potential for producing ceramic materials of designed composition and properties. A typical sol-gel process involves the hydrolysis and polymerization of one or more metal alkoxides in an alcohol solution in a batch reactor to form a homogeneous gel, which is then further treated to provide the type of ceramic desired (aerogel, glass, crystal, coating, etc.).

Several authors have suggested that diffusion effects may influence the development of the gel microstructure. To investigate if diffusion effects are important, we begin by determining what governs the diffusivity of the precursors using the pulsed-gradient-spin-echo NMR technique. This report focuses on the early stages of the batch reaction.

The system chosen is the acid catalyzed hydrolysis and condensation of tetraethyl orthosilicate (TEOS) in ethanol. Our results from ^{1}H PGSE NMR and ^{29}Si NMR show that the diffusivities of the silicate precursors are not just a function of the molecular weight. Hydrogen bonding between the polar functional groups and the solvent also decreases the mobility of the reactants. Moreover, since hydrolysis increases and polymerization reduces the concentration of these polar groups, the mobility of the reactive oligomers changes in a complex manner. Combining our results from PGSE NMR and gas chromatography, we estimate the extent of hydrogen bonding effect on the mobility of various oligomers, providing a model to predict diffusivity trends throughout the batch reaction.

INTRODUCTION

The hydrolysis and condensation of TEOS in alcohol is one of the most extensively studied systems in sol-gel synthesis. Previous work has focused on the reaction mechanisms, the kinetics, the structure and mechanism of growth, and the effects of processing parameters (for an excellent review, see ref. 1). Typical reactions are:

Hydrolysis

$$(EtO)_3Si\text{-}OEt \ + \ H_2O \ \rightarrow \ (EtO)_3Si\text{-}OH \ + \ EtOH \tag{1}$$

Condensation

$$(EtO)_3Si\text{-}OEt \ + \ HO\text{-}Si(OEt)_3 \ \rightarrow \ (EtO)_3Si\text{-}O\text{-}Si(OEt)_3 \ + \ EtOH \tag{2}$$

$$(EtO)_3Si\text{-}OH \ + \ HO\text{-}Si(OEt)_3 \ \rightarrow \ (EtO)_3Si\text{-}O\text{-}Si(OEt)_3 \ + \ H_2O \tag{3}$$

where Et represents CH_2CH_3. The reactions above represent only a few generic reactions. The entire sol-gel synthesis process involves many reactants and products ranging from monomers to large polymers, each with various degrees of hydrolysis.

X-ray scattering studies [2-5] have shown that, depending on processing conditions (e.g. type of catalyst, water concentration, etc.), the condensation reactions can lead to radically different gel structures - from colloidal particles to weakly branched polymeric networks. Results obtained by Himmel and coworkers [3] show that the fractal dimension of the gels decreases with decreasing starting water concentration and solution pH (for pH values less than 2). Consistent with other results [4,5], gels produced with low water concentration at low pH were found to be weakly branched.

Computer simulations [6] on the growth of fractal objects have shown that the fractal dimension can depend on the nature of the growth process (e.g. particle-cluster vs. cluster-cluster growth) and the rate-determining step (e.g. reaction-limited vs. diffusion-limited). Comparing their results with computer simulations, Himmel and others suggest that the weakly branched gel produced from the hydrolysis and condensation of TEOS with low water concentration and solution pH is a result of a diffusion-limited growth process.

Pouxviel and Boilot [7] have found that even though initially the system with water-to-silicon molar ratio (r_W) of 10 showed faster hydrolysis rate and higher degree of condensation than the system with $r_W = 4$, the former takes about twice as long to gel. To explain this apparent inconsistency in kinetic behavior, they speculate that the growth process changes from kinetic- to diffusion-controlled as the polymers become sufficiently large, at which point the diffusion-controlled growth is then faster for the system with smaller polymers (i.e. $r_W = 4$). Colby and coworkers [8] compared the gel time of an HCl-catalyzed TEOS system with a similar TMOS (tetramethyl orthosilicate) system, and found that the apparent activation energy for gelation was higher for the TEOS system. The difference was attributed by these workers to the effects of diffusion.

The origin of different gel structures is still not well understood. In particular, it is not clear how diffusion limitations can play a role in the microstructural development of the gels. By understanding factors controlling diffusion, it is possible to engineer the properties of sol-gel derived materials. In this work, we investigate the factors that govern the mobility of intermediates. It is to be expected that changes in diffusivity might be more complicated than in ordinary polymer solutions since molecular weight, solvent polarity, and polymer group polarity are changing simultaneously in a batch reactor.

EXPERIMENTS

1. Preparation of the TEOS reaction mixture

TEOS and absolute ethanol (both used as purchased from Aldrich and Minnesota Grain Products, respectively) were mixed slowly for 20 seconds. Aqueous acid solution was added, with vigorous stirring, for 1 minute to yield a solution with the molar composition TEOS : EtOH : H_2O : HCl = 1 : 4 : 0.8 : 0.0008 (the selection of this system will be discussed later). The sample was kept at room temperature and remained clear over the reaction times studied (from 1 hour to 27 days). Samples were prepared with a range of reaction times and were analyzed together on the same day so that signal intensities could be compared quantitatively between spectra without variations introduced by probe tuning, magnet shimming, etc.. Three separate sets of data were obtained to estimate the reproducibility of the diffusion results.

2. ^1H and ^{29}Si NMR

^1H spectra were obtained on a Nicolet NT300 at 300 MHz and ^{29}Si spectra on a Varian VXR500 at 99.3 MHz. Chromium(III) acetylacetonate was used as a paramagnetic relaxing agent to reduce the T_1 of ^{29}Si to about 2.5 seconds. For each ^{29}Si spectrum, a total of 1024 scans separated by a relaxation delay of 3 seconds, and a line-broadening of 1.0 Hz were employed. To check if the fast relaxation delay affect the quantitative nature of the spectra, we compared the integrated peak intensities of these spectra with those where an ample relaxation delay of 12 seconds was used (Figures 8 and 13); we have found no significant difference.

3. PGSE NMR experiment

The pulsed-gradient-spin-echo NMR technique is used to determine the self-diffusion coefficient of intermediates oligomers. The technique involves labeling the positions of nuclei by applying a magnetic field with a spatial gradient. It is a non-intrusive method and ideal for probing the thermal motion of chemical species. The technique is standard for studies in polymer solutions and melts [e.g., 9-12] and emulsions [e.g., 13]. Detailed descriptions of the PGSE NMR technique can be found in several sources [9,10,13,14], which explain that the self-diffusion coefficient, D, of a chemical species is related to its NMR signal intensity, S, by the following equation [10]:

$$S = S_0 \exp(-2\Delta/T_2) \exp(-\gamma^2 G^2 \beta D) \qquad (4)$$

where,

$$\beta = \delta^2(\Delta - \delta/3), \qquad (5)$$

T_2 = the spin-spin relaxation time constant

G = the field gradient strength, in units of $Tesla \cdot cm^{-1}$

Δ = the diffusion observation time

δ = the duration of the pulsed gradient

γ = the nucleus gyromagnetic ratio, in units of $rad \cdot Tesla^{-1} \cdot s^{-1}$

PGSE experiments were performed on a Nicolet 300 MHz NMR spectrometer with parameters:

$$\Delta = 100 \text{ ms}$$
$$\delta = 0.4 \text{ ms to } 5.4 \text{ ms}$$
$$G \approx 15 \text{ Gauss/cm} = 0.15 \text{ Tesla/m}$$

For self-diffusion coefficients in the order of $10^{-5} cm^2/s$, an observation time of $\Delta = 100$ ms is recommended [15]. This corresponds to a root-mean-square displacement of:

$$\sqrt{<(r-r_0)^2>} = \sqrt{6D\Delta} \approx 20 \mu \qquad (6)$$

The field gradient strength was calibrated using benzene at 25 °C ($2.28 \times 10^{-5} cm^2/s$). For each self-diffusion measurement, 10 to 26 values of δ were used, holding Δ constant. In accordance with equation 4, the self-diffusion coefficient D of the silicate oligomers was found by plotting $\ln(S)$ versus β, where S is the integrated proton signal intensity of the ($-SiO-CH_2$) group.

4. Gas Chromatography

An experimental study of molecular motion in a multi-component system must include the identification of various molecules and the determination of their concentrations. These

molecules are the various silicate oligomers (e.g. monomers, dimers, trimers, etc.), the distribution of which cannot be accurately determined solely by NMR. Combining data from gas chromatography and ^{29}Si NMR, though, we were able to separate and identify the silicate oligomers. These techniques have been used by other investigators [16-18] for studies on the hydrolysis and condensation of TMOS (tetramethyl orthosilicate).

Flame ionization detection was effective in detecting and quantifying hydrocarbon-containing molecules [19]. It has been referred to as a carbon-counting device since the response factor for a molecule is approximately proportional to the number of carbon it contains (comparison of GC-FID peak intensities with ^{29}Si NMR results showed that the approximation is reasonable). We were able to quantify the molecular size distribution using this technique since our system does not contain completely hydrolyzed silicates, as verified by ^{29}Si NMR.

The GC-FID used was a Hewlett Packard HP 5890 series II. A 10 m x 0.53 mm i.d. fused silica capillary column bonded with 50% phenyl and 50% methyl-polysiloxane, film thickness 2.0 μm (Hewlett Packard model HP-17), is employed using helium as carrier gas. The operating conditions, following [17], were:

injector temperature = 300 °C
detector temperature = 300 °C
oven temperature program:
    60 °C for 1 minute
    15 °C/min to 150 °C
    5 °C/min to 260 °C
    260 °C for 1 minute.
column flow rate = 22 ml/min

Figure 4
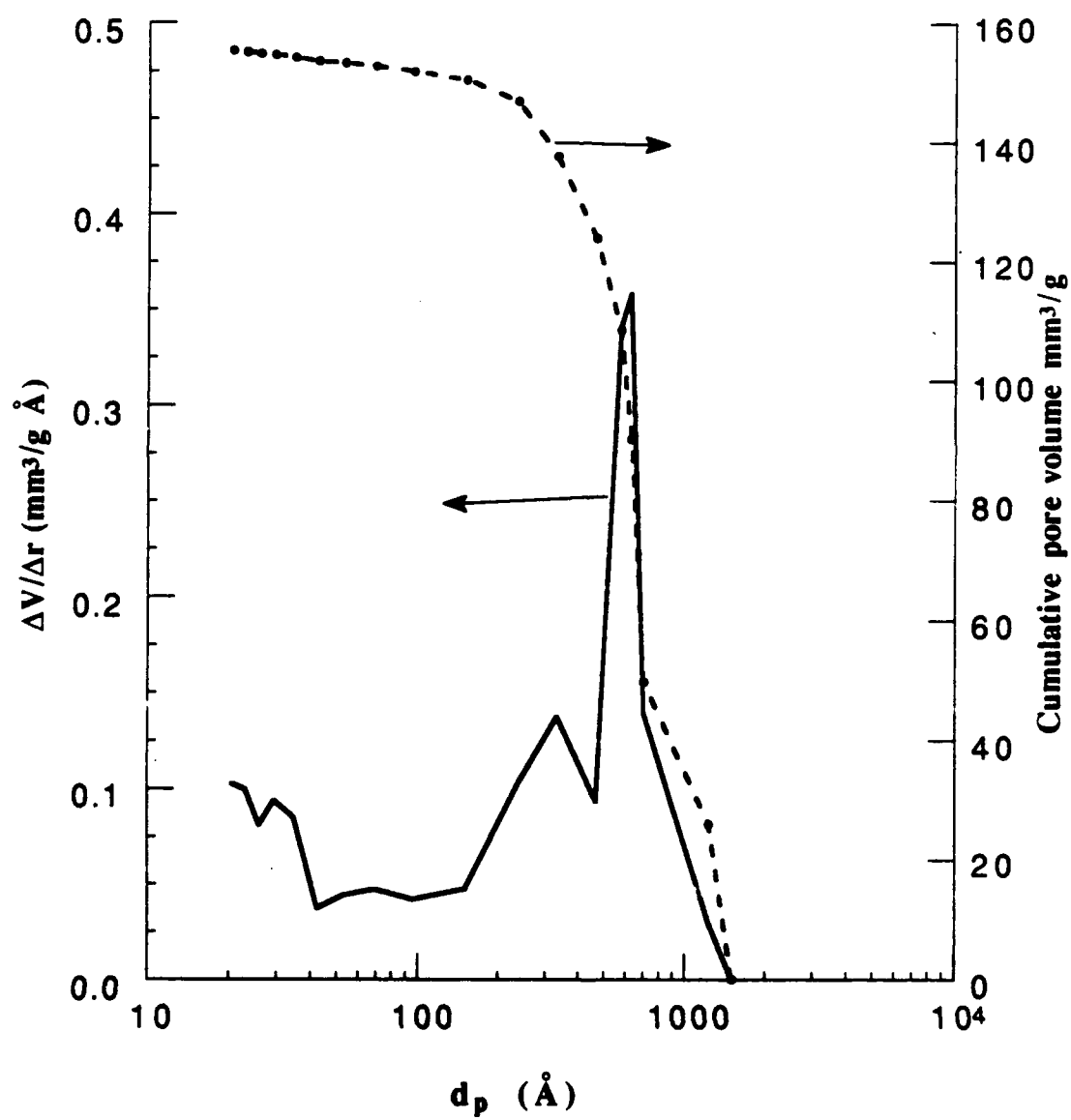
RESULTS AND DISCUSSION

A. Selection of Composition

A typical proton NMR spectrum for the reaction mixture is shown in Figure 1. Note that because of fast chemical exchange, the (-OH) peak is a mole-weighted average of the signals from the protons of water, the hydroxyl groups on ethanol and silanols. The phenomenon of fast chemical exchange occurs because the nuclei are rapidly exchanging between various molecular sites, with respect to the NMR detection time. As the exchange slows down, the individual peaks will be resolved. This effect can be seen on a ^{1}H spectrum of a mixture of TEOS, ethanol and water (Figure 2). The exchange slows down without the acid, which catalyzes proton exchange [20]. Note that a ^{1}H spectrum (Figure 3) with higher water concentration confirms the water peak identification. High water concentration promotes proton exchanges, as shown by the collapse of ethanol hydroxyl triplet.

Another feature of the ^{1}H spectra is that protons on all silicon-bonded ethoxy groups resonate at virtually the same frequency. This means that various silicate species, e.g. monomers, dimers, etc., cannot be differentiated through the proton signals on the NT300 (a 300 MHz spectrometer) [21]. Moreover, the methyl signal on the silicate overlaps with that on the ethanol. Since the (-SiO-CH$_2$) signal is the only one available for the labeling of the various silicate species, the self-diffusion coefficient measured is an average of all ethoxy-containing silicates. In order to preserve this signal for the PGSE experiments, we are restricted to systems with low concentration of water because, when present in high concentration, water promotes hydrolysis which replaces the ethoxy groups, as shown in Figure 4. These systems also tend to yield weakly-branched polymers which, simulations suggest, are formed by a diffusion-limited process. Further work is underway using "tagging" silylation technique.

B. Self-diffusion of silicate intermediates

Figure 5 shows that the plot of ln(S) versus β, from which the average self-diffusion coefficient of the ethoxy-containing silicates is obtained, is a straight line, suggesting that polydispersity in the silicate mobility is negligible [22]. The change in the silicate mobility with reaction is shown in Figure 6.

The observed initial decrease in mobility is consistent with the expected increasing average molecular weight of the silicates. The most striking feature of the diffusion data is that, rather than continuing to decrease, the average mobility of the ethoxy-containing silicates levels off, and then rises slightly, even though we expect that the molecular weight continues to increase. This anomaly suggests that there are factors other than the molecular weight which determine the silicates mobility.

To reveal other factors affecting the mobility of the silicates, ^{29}Si NMR is used.

C. The effect of molecular weight

1. ^{29}Si NMR

The peak assignments for the ^{29}Si NMR spectra, displayed in Figure 7, follow those reported in the literature [21(b),23,24]. The chemical shifts of commercial products TEOS and ethyl polysilicates are known. The latter exhibits three lines corresponding to the end, middle and trisubstituted groups. In addition, since a hydroxyl substituent on the silicon nucleus is more electron-withdrawing than an ethoxy substituent, a shift of +2.5 ppm for each replacement of an ethoxy group by a hydroxyl group has been shown [21(b)]. The assignments of the unhydrolyzed middle-group silicon in a cyclic tetramer (approx. -95 ppm) and a linear oligomer (approx. -96 ppm) follow the results obtained by Marsmann and coworkers [25]. The strained bond-angle in a cyclic tetramer causes a slight deshielding effect. This trend is also observed by Harris and Knight who identified the ^{29}Si chemical shifts of the silicate ions in alkaline aqueous potassium silicate solutions [26]. Note that no cyclic trimers are found (the unhydrolyzed and completely hydrolyzed species resonate at -87.97 ppm [25] and -82.9 ppm [27], respectively).
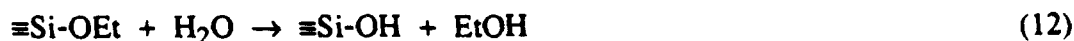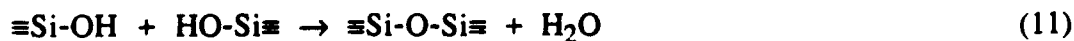
The multiplets for (SiO)-$\underline{Si}$-$(OH)(OEt)_2$, (SiO)-$\underline{Si}$-$(OEt)_3$ and linear $(SiO)_2$-$\underline{Si}$-$(OEt)_2$ sites are due to the variety of different environment of the adjacent silicon. Hydrolysis of the adjacent silicon causes deshielding, while substitution on this silicon causes shielding. Peak intensity comparisons of several spectra, combined with results from GC-FID, lead to the more detailed assignments shown in Figure 8. These assignments agree with those reported by Kelts and Armstrong [24].

It can be seen from the ^{29}Si NMR spectra (Figure 7) that all the silicons are linked to ethoxy groups, so that they are accounted for in the diffusion and GC-FID measurements. To examine the evolution of different silicon sites, the peaks are integrated, and the intensities plotted against reaction time in Figure 9.

From Figure 9, it appears that, between 0 and 20 hours, a high concentration of the monohydrolyzed monomers ($Si(OEt)_3(OH)$) is formed, and quickly condensed, resulting in high concentration of endgroups (SiO)-$Si(OEt)_3$. A combination of hydrolysis and condensation also results in (SiO)-$Si(OEt)_2(OH)$. These hydrolyzed endgroups undergo further condensation, leading to the disubstituted silicons ($(SiO)_2$-$Si(OEt)_2$). The liberated water hydrolyzes the remaining endgroups, resulting in further condensation. The reactions can be represented as (R can be Et or H):

$$Si(OEt)_4 + H_2O \rightarrow (HO)\text{-}Si\text{-}(OEt)_3 + EtOH \tag{7}$$

$$\equiv Si\text{-}OR + HO\text{-}Si\text{-}(OEt)_3 \rightarrow \equiv Si\text{-}O\text{-}Si(OEt)_3 + ROH \tag{8}$$

$$\equiv Si\text{-}OR + (HO)_2\text{-}Si\text{-}(OEt)_2 \rightarrow \equiv Si\text{-}O\text{-}Si(OH)(OEt)_2 + ROH \tag{9}$$

$$\equiv Si\text{-}O\text{-}Si(OH)(OEt)_2 + RO\text{-}Si\equiv \rightarrow (\equiv Si\text{-}O)_2\text{-}Si(OEt)_2 + ROH \tag{10}$$
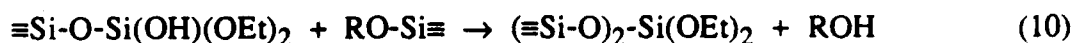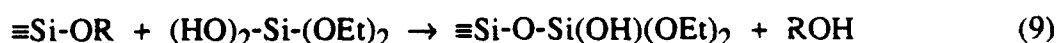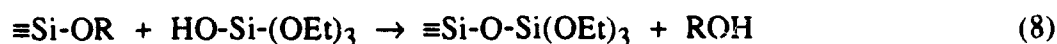
When the concentration of water and silanols drop (time > 200 hours), the rates of hydrolysis and condensation should become comparable. Consequently, as shown by the following equations, the concentration of silanol decreases only slowly:

$$\equiv Si\text{-}OH + HO\text{-}Si\equiv \rightarrow \equiv Si\text{-}O\text{-}Si\equiv + H_2O \tag{11}$$

$$\equiv Si\text{-}OEt + H_2O \rightarrow \equiv Si\text{-}OH + EtOH \tag{12}$$

It is clear from Figure 9 that condensation continues throughout the experiments, as shown by the increase in concentration of the disubstituted silicon groups and by the decreasing proportion of (SiO)-$\underline{Si}$(OEt)$_2$(OH). Since the (SiO)-$\underline{Si}$(OEt)$_3$ sites are present in much higher concentration than the (SiO)-$\underline{Si}$(OEt)$_2$(OH) sites, the condensation observed here will most likely result in short chain oligomers (chances of termination is high). Moreover, since the degree of hydrolysis is low, the oligomers are probably linear. These observations are supported by the results of GC-FID.

2. Gas Chromatography

Gas chromatograms are shown in Figure 10, where the peak assignments are aided by the results of Klemperer and coworkers [17,28] as well as the ^{29}Si NMR results. Similar oligomers have been detected for systems with the same range of water-to-silicon ratio [29]. It has been found [28] that the presence of hydroxyl groups on an oligomer increases the species retention time slightly. This is understandable since the hydroxyl groups promote hydrogen bonding which will lower the vapor pressure.

The mole fractions of the silicon oligomers are calculated from the peak intensities, and are shown in Figure 11. These results show that reactions are occurring rapidly within the first few hours after mixing, leading to the sequential formation of hydrolyzed monomers, dimers and trimers. The reaction rates slow markedly after 24 hours, but condensation is still occurring. Note that beyond a certain point, all reactions have ceased, so that there is no observable change between the gas chromatograms for the 4-month and 9-month samples.
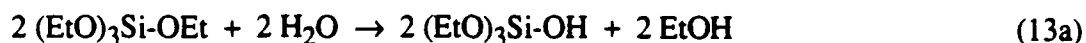
D. Hydrogen Bonding

1. Small oligomers

It is clear that some factor other than molecular weight is decreasing the average mobility of the silicates. The solvent is a mixture of water and ethanol, containing polar hydrogen atoms which are ready to form hydrogen bonds with the hydroxyl groups of the silanols. The mobility of these solutes will consequently decrease [30-32]. The effect of hydrogen bonding on the solute mobility has been reported for some polymeric systems [33].

One indication of the H-bonding effect is the drastic drop in the silicate mobility one hour after mixing, when chromatograms show that low molecular weight silanols are present in high concentrations. After 24 hours, GC-FID and ^{29}Si NMR (Figure 9) both show that the reaction mixture still contains a high concentration of silanols, so the silicate mobility stays rather constant owing to the solute-solvent associations effect. Eventually, when the silanols are consumed completely, a rise in silicate mobility is observed. The loss in silicon hydroxyl groups is also coincidental with the complete consumption of water (Figure 12). Without any water, reactions stop at this point, leaving predominantly dimers and trimers (Figure 10) with an average diffusion coefficient of 0.60×10^{-5} cm^2/s.

The consumption of water is a net result of the hydrolysis and condensation of TEOS, as shown by the following stoichiometric relations:

$$2 \, (EtO)_3Si\text{-}OEt \; + \; 2 \, H_2O \; \rightarrow \; 2 \, (EtO)_3Si\text{-}OH \; + \; 2 \, EtOH \qquad (13a)$$
$$2 \, (EtO)_3Si\text{-}OH \; \rightarrow \; (EtO)_3Si\text{-}O\text{-}Si(OEt)_3 \; + \; H_2O \qquad (13b)$$
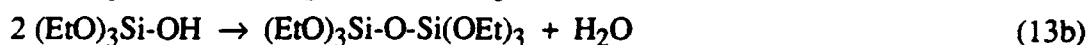
The equation above indicates that water is gradually consumed and ethanol produced as reactions progress. The system starts with low water concentration (a substoichiometric water-to-silicon molar ratio, W/Si, of 0.8), so that the water supply for the reactions vanishes before an appreciable degree of polymerization is achieved. It is shown in Appendix A how the water and ethanol content of the system can be calculated from the ^{29}Si NMR results using molar balances.

The effect of H-bonding in reducing the mobility of silicon precursors can no doubt be better demonstrated by studying systems with high degree of hydrolysis. However, this plan is limited, at present, by experimental considerations since we must retain the silicon-bonded ethoxy group for NMR labeling. Even for systems which undergo limited hydrolysis, the rate of reaction must be slow enough so that diffusion measurements, which typically runs for about 7 minutes for one result, can be performed. However, there is hope of "tagging" large, fully hydrolyzed polymers with a trimethylsilylating reagent [34].

To examine the effect of H-bonding more closely, the extent of hydrolysis on intermediate silicon oligomers can be increased by first preparing incompletely hydrolyzed oligomers and then hydrolyzing them with additional water.

2. Intermediate oligomers

As shown earlier, a system with low water concentration produces only silicon oligomers, all containing ethoxy groups. To such a system, addition of limited amount of water at the end of the reaction should again initiate hydrolysis but without losing all the ethoxy groups for diffusion measurements. Moreover, since hydrolysis is occurring with silicon oligomers, the rate of reaction is slower than if it is with monomers [7,35], and the conditions are more closely related to those in our previous experiment.

To produce the initial silicon oligomers, a system with molar composition TEOS : EtOH : H_2O : HCl = 1 : 4 : 0.5 : 0.0005 is prepared. The sample is then allowed to react for about 3 months (the ^{29}Si NMR spectrum, shown in Figure 13, for a 1-month-old sample shows that reactions have virtually ceased, leaving monomers, dimers and trimers). To the 3-month-old sample, limited amounts of water (total W/Si = 0.8 and 1.0) are added, and ordinary ^{1}H NMR and PGSE NMR experiments are performed. To estimate the extent of hydrolysis (without resorting to ^{29}Si NMR), the molar ratio of the silicon-bonded ethoxy groups to ethanol $\left[\dfrac{-SiO-CH_2^{*}-}{HO-CH_2^{*}-} \right]$ is obtained from the ^{1}H NMR spectra. Hydrolysis leads to a drop in the concentration of the ethoxy group and a rise in ethanol concentration. Consequently, the extent of initial hydrolysis is reflected by the drop in the $\left[\dfrac{-SiO-CH_2^{*}-}{HO-CH_2^{*}-} \right]$ molar ratio. This ratio levels off when hydrolysis slows down and condensation becomes significant, and so this ratio characterizes the amount of hydrolyzed groups present. Hence, by monitoring and comparing the $\left[\dfrac{-SiO-CH_2^{*}-}{HO-CH_2^{*}-} \right]$ molar ratio and the silicate average mobility, the effect of H-bonding can be examined (Figure 14).

The initial drop in the average mobility follows the extent of hydrolysis consistently for both systems. The initial larger drop in mobility for the system with higher water concentration is consistent with a higher degree of hydrolysis. As hydrolysis slows down and condensation speeds up, the average mobility rises - a trend similar to the one observed in previous experiment. Notice that with the loss of hydrogen bonding, the difference in mobility between the two systems becomes smaller. This indicates that, at least for low molecular weight systems, the effect of hydrogen bonding is more significant than the molecular weight effect.

Results from the diffusion experiments have shown that the diffusivity of silicon precursors is reduced both by the increase in their molecular weight and the degree of hydrolysis, the latter is due to hydrogen bonding with the solvent molecules. The extent of these two factors can be seen by comparing the estimated diffusivities of the hydrolyzed and unhydrolyzed species.

E. Diffusivity of Hydrolyzed and Non-Hydrolyzed Oligomers

The average diffusion coefficient measured by ^{1}H PGSE NMR experiments at any time is related to the self-diffusion coefficient of the silicon oligomers by the following equation:

$$D_{av} = \sum_{j=1}^{m} f_j^{eth} D_j \tag{14}$$

where f_j^{eth} is the fraction of ethoxy belonging to the j-mer (the oligomer containing j silicon) and can be obtained from the gas chromatograms since the GC-FID peak intensity is proportional to the number of carbon in the molecule. Thus,

$$f_j^{eth} = \frac{(\%Area)_j}{\sum_{k=1}^{m}(\%Area)_k} \tag{15}$$

where $(\%Area)_j$ is the percent integrated peak area for species j. Between 10 and 40 hours, the species that are present in significant amount are monomer, monohydrolyzed monomer, dimer, monohydrolyzed dimer, trimer and monohydrolyzed trimer. To extract the diffusion coefficients of these species from the average value, we need to solve a set of 6-by-6 linear equations. Since we presume that the monomer diffusivity is the average diffusivity obtained at time t = 0, we only need 5 more data sets. The percent peak area in equation (15) and the average diffusivities are extracted from the curves drawn through the corresponding data. The linear equation set is solved using the method of Gaussian elimination with partial pivoting [36], and the results are shown in Table 1 and plotted in Figure 15. The Stokes-Einstein hydrodynamic radii are estimated using a pure ethanol solvent viscosity of 1.1 cP obtained from the literature [32].

Table 1:   Diffusivity and Hydrodynamic Radii of Silicon Oligomers

Oligomer	Diffusivity [a] [10^{-5} cm^2/s]	Hydrodynamic Radius [Å]
monomer	0.900	2.206
dimer	0.591	3.360
trimer	0.521	3.810
linear tetramer [b]	0.500	3.971
monohydrolyzed monomer	0.447	4.441
monohydrolyzed dimer	0.176	11.283
monohydrolyzed trimer[b]	0.100	19.850

[a] The error is estimated to be ± 0.03 based on the deviation on the average diffusivity.

[b] From extrapolation.

Note that the diffusivities above are estimated based on the average diffusivities measured when the water concentration is still high. Complexation with the water molecules reduces the diffusivities of the hydrolyzed species by increasing the effective hydrodynamic radii. At this stage of the reaction, molecular weight plays a lesser role in determining the diffusivity of the oligomers.

The hydrogen bonding effect in reducing the mobility of the silicon species has been demonstrated. Nevertheless, the consequences of H-bonding are far-reaching. The effects of H-bonding on chemical reaction rates have been observed [37]. Moreover, according to the absolute reaction rate theory [38], H-bonding can reduce the condensation reaction rate constant by increasing the heat of activation. This effect suggests that condensation is more favorable in aprotic solvents. It also suggests that alcohol-producing condensation reaction is thermodynamically more favorable than water-producing condensation since the latter involves two water-complexed reactants. The effects of hydrogen bonding on the condensation process in sol-gel reactions have been discussed in the literature [39].

Comparing our diffusion results with the kinetic studies performed separately in our group, the Smoluchowski equation [40] predicts that the early stages of condensation reactions (i.e. when the Brownian motion of the reactants is not hindered) are reaction-limited. However, when the polymers become sufficiently large, diffusion effects can be

important.   The influence of diffusion on the overall reaction rate and the polymer microstructural development is presently being examined.

SUMMARY

It has been suggested in the sol-gel literature that diffusion effects may influence the development of the gel microstructure. To investigate if diffusion effects are important, we begin by determining what governs the diffusivity of the precursors

This work focuses on the early stages of the sol-gel reaction by studying the acid-catalyzed hydrolysis and condensation of TEOS with starting molar ratio TEOS : Ethanol : H_2O : HCl $= 1 : 4 : 0.8 : 0.0008$ using ^1H, ^{29}Si and ^1H-PGSE NMR, and gas chromatography with flame ionization detector. Low molecular weight, partially hydrolyzed oligomers (mainly dimers) are formed rapidly and the average mobility of these silicates decreases from 0.90×10^{-5} cm^2/s (monomer diffusivity) to an average value of 0.56×10^{-5} cm^2/s. As condensation continues, shown by ^{29}Si NMR and GC-FID, the average mobility remains around this value up to 250 hours and then goes up slightly to 0.60×10^{-5} cm^2/s. Our results show that the mobility of the silicon precursors is reduced with increasing molecular weight and the extent of hydrolysis. Complexation with the water molecules reduces the diffusivities of the hydrolyzed species by increasing the effective hydrodynamic radii. At early stage of the reaction, molecular weight plays a lesser role in determining the diffusivity of the oligomers. We attribute the late rise in mobility to the loss in hydrogen bonding as silanols and water are consumed completely. Reactions have stopped without water so that our system produces only low molecular weight oligomers, the largest detected in significant amount being the linear tetramers. Although the early stages of reactions are clearly not diffusion-limited, our results suggest that hydrogen bonding may be important in slowing the motion of intermediates in the presence of high water concentration.

These results have demonstrated that unlike ordinary polymer solutions, the diffusivity of sol-gel intermediates depends on a combination of molecular weight, solvent polarity, and polymer group polarity, the contribution of each of these factors changes with the extent of reaction.

REFERENCES

1. C.J. Brinker and G.W. Scherer, <u>Sol-Gel Science. The Physics and Chemistry of Sol-Gel Processing</u>, Academic Press, Inc. (1990)

2. D.W. Schaefer and K.D. Keefer, <u>Mat. Res. Soc. Symp. Proc.</u>, <u>73</u>, 277-288 (1986)

3. B. Himmel, Th. Gerber and H. Burger, <u>JNCS</u>, <u>119</u>,1-13 (1990)

4. C.J. Brinker, K.D. Keefer, D.W. Schaefer, R.A. Assink, B.D. Kay and C.S. Ashley, <u>JNCS</u>, <u>63</u>, 45-59 (1984)

5. D.W. Schaefer and K.D. Keefer, <u>Mat. Res. Soc. Symp. Proc.</u>, <u>32</u>, 1-14 (1984)

6. see references in 1, 2 and 3.

7. J.C. Pouxviel and J.P. Boilot, <u>JNCS</u>, <u>94</u>(3), 374-386 (1987)

8. M.W. Colby, A. Osaka and J.D. MacKenzie, <u>JNCS</u>, <u>99</u>, 129-139 (1988)

9. E.D. von Meerwall, <u>Advances in Polymer Science</u>, <u>54</u>, 1-29 (1983)

10. F.D. Blum, <u>Spectroscopy</u>, <u>1</u>(5), 32-38 (1986).

11. B.D. Boss, E.O. Stejskal and J.D. Ferry, <u>J. Phys. Chem.</u>, <u>71</u>(5), 1501-1506 (1967)

12. D.W. McCall, D.C. Douglass and E.W. Anderson, <u>J. Polym. Sci.: A</u>, <u>1</u>, 1709-1720 (1963)

13. P. Stilbs, <u>Progress in NMR Spectroscopy</u>, <u>19</u>, 1-45 (1987)

14. P.T. Callaghan, <u>Aust. J. Phys.</u>, <u>37</u>, 359-87 (1984)

15. PFG NMR User's Manual, NMR Laboratory, Chemistry Department, University of Minnesota.

16. G. Wheeler, <u>Ultrastructure Processing of Advanced Ceramics</u>, J.D. MacKenzie and D.R. Ulrich (eds.) (1988)

17. W.G. Klemperer, V.V. Mainz, S.D. Ramamurthi and F.S. Rosenberg, <u>Mat. Res. Soc. Symp. Proc.</u>, <u>121</u>, 15-24 (1988)

18. W.G. Klemperer and S.D. Ramamurthi, <u>Mat. Res. Soc. Symp. Proc.</u>, <u>121</u>, 1-13 (1988)

19. D.J. David, Gas Chromatography Detectors, John Wiley and Sons (1974)

20. E.D. Becker, <u>High Resolution NMR</u>, NY: Academic Press (1969)

21 The overlapping of the signals on a 270 MHz spectrometer had been reported [a] (our experience with a 500 MHz spectrometer is also similar). Results of previous workers and ours are inconsistent with those reported by Turner and Franklin who used a 90 MHz Bruker [b].

(a)   J.E. McGrath, J.P. Pullockaren, J.S. Riffle, S. Kilic and C.S. Elsbernd, Ultrastructure Processing of Advanced Ceramics, J.D. MacKenzie and D.R. Ulrich (eds.) (1988)
(b)   C.W. Turner and K.J. Franklin, JNCS, 91, 402-415 (1987)

22   E.D. von Meerwall, J. Mag. Res., 50, 409-416 (1982)

23.   J.C. Pouxviel, J.P. Boilot, J.C. Beloeil and J.Y. Lallemand, JNCS, 89, 345-360 (1987)

24.   L.W. Kelts and N.J. Armstrong, J. Mater. Res., 4(2), 423-433 (1989)

25.   H.C. Marsmann, E. Meyer, M. Vongehr and E.F. Weber, Makromol. Chem., 184, 1817-1822 (1983)

26.   R.K. Harris and C.T.G. Knight, J. Chem. Soc. Faraday Trans. 2, 79, 1525-1561 (1983)

27.   Von G. Engelhardt, W. Altenburg, D. Hoebbel and W. Wieker, Z. anorg. allg. Chem., 428, 43-52 (1977)

28.   W.G. Klemperer and S.D. Ramamurthi, Polym. Prepr., Am. Chem. Soc. Div. Polym. Chem., 28, 432-433 (1987)

29.   C.A.M. Mulder and A.A.J.M. Damen, JNCS, 93, 169-178 (1987)

30.   G.C. Pimentel and A.L. McClellan, The Hydrogen Bond, W.H. Freeman and Company (1960)

31.   S.N. Vinogradov and R.H. Linnell, Hydrogen Bonding, Van Nostrand Reinhold Company (1971)

32.   Tibor Erdey-Gruz, Transport Phenomena in Aqueous Solutions, John Wiley & Sons (1974)

33.   I.J. Mokrys, D. Rigby and R.F.T. Stepto, Ber. Bunsenges. Phys. Chem., 83, 446-454 (1979)

34.   A.E. Pierce, Silylation of Organic Compounds, a technique for gas-phase analysis, Pierce Chemical Company, Illinois (1968)

35.   J. Sanchez and A.V. McCormick, in press.

36.   G.E. Forsythe, M.A. Malcolm and C.B. Moler, Computer Methods for Mathematical Computations, Prentice-Hall, Inc., NJ (1977)

37.   E.S. Amis and J.F. Hinton, Solvent Effects on Chemical Phenomena, v.1, Academic Press (1973)

38.   K.J. Laidler, Chemical Kinetics, 2nd. ed., McGraw-Hill Book Company (1965)

39.   I. Artaki, T.W. Zerda and J. Jonas, JNCS, 81, 381-395 (1986)

40.   E.L. Cussler, Diffusion, Mass transfer in fluid systems, Cambridge University Press (1984)

Appendix A

Water and Ethanol Content

From equations (1), (2) and (3), we observe that, in the hydrolysis and condensation of TEOS, the proton (H) and ethyl (Et) groups are neither created nor destroyed. Hence, the total concentration of each of these groups is conserved. A molar balance on (Et-) shows that the ethanol concentration at any time (expressed in molar ratio of ethanol-to-silicon) is related to the concentrations of various silicon-groups as determined from the ^{29}Si NMR spectra in Figure 9 (all quantities, in bold letters, are expressed as ratios to the total concentration of silicons, subscript zero indicates initial value):

$$\textbf{Et-OH} + \textbf{EtO-Si} = \textbf{(Et-)}_0 \qquad \text{(A-1)}$$

$$\begin{aligned} \textbf{EtO-Si} = 3\left[\textbf{(EtO)}_3\textbf{-Si-OH}\right] &+ 4\left[\textbf{(EtO)}_4\textbf{-Si}\right] \\ &+ 2\left[\textbf{(EtO)}_2\textbf{(OH)-Si-(OSi)}\right] + 3\left[\textbf{(EtO)}_3\textbf{-Si-(OSi)}\right] + 2\left[\textbf{(EtO)}_2\textbf{-Si-(OSi)}_2\right] \end{aligned}$$
$$\text{(A-2)}$$

From the starting composition, the initial concentration of the ethyl group is 8. Similarly, the water concentration at any time can be determined from a molar balance of (H-), as shown below:

$$\textbf{H}_2\textbf{O} + \textbf{EtOH} + \textbf{Si-OH} = \textbf{(H-)}_0 \qquad \text{(A-3)}$$

$$\textbf{Si-OH} = \left[\textbf{(EtO)}_3\textbf{-Si-OH}\right] + \left[\textbf{(EtO)}_2\textbf{(OH)-Si-(OSi)}\right] \qquad \text{(A-4)}$$

The value of **EtOH** in equation (A-3) can be obtained from equations (A-1) and (A-2), while the initial concentration of (H-) is 5.6. The concentration of water is then equal to $\frac{1}{2}\left[\textbf{H}_2\textbf{O}\right]$. Figure 12 shows the calculated results.

FIGURE CAPTIONS

1. A typical ^{1}H spectrum (ref. TMS) for a reaction mixture of TEOS, ethanol, water and HCl.
   molar ratio TEOS : EtOH : H_2O : HCl = 1 : 4 : 0.8 : 0.0008
   reaction time = 655 hours ($\approx$27 days)

2. A ^{1}H spectrum for a mixture of TEOS, ethanol and water.
   molar ratio TEOS : EtOH : H_2O = 1 : 4 : 0.8
   The spectrum was obtained within about 0.5 hour.
   No reaction could have occurred appreciably.

3. A ^{1}H spectrum for a mixture of TEOS, ethanol and water.
   molar ratio TEOS : EtOH : H_2O = 1 : 4 : 4
   The spectrum was obtained within about 1 hour.
   No reaction could have occurred appreciably.

4. A ^{1}H spectrum for a reaction mixture of TEOS, ethanol, high water concentration and HCl.
   molar ratio TEOS : EtOH : H_2O : HCl = 1 : 4 : 4 : 0.0005
   reaction time = 26 hours
   High water concentration results in significant extent of hydrolysis, and thus the disappearance of silicon-bonded ethoxy signals.

5. Determination of self-diffusion coefficient from the slope of a plot of ln(S) versus β, where S is the (-SiO-CH_2-) peak integral and β is as defined in equation (5).
   molar ratio TEOS : EtOH : H_2O : HCl = 1 : 4 : 0.8 : 0.0008

6. Mobility of silicates in TEOS hydrolysis and condensation as determined by ^{1}H PGSE NMR
   molar ratio TEOS : EtOH : H_2O : HCl = 1 : 4 : 0.8 : 0.0008
   The deviation of the curve is estimated to be $\pm$ 0.03 cm^2/s,
   based on the data for t $\approx$ 180 h.

   * molar ratio TEOS : EtOH : H_2O = 1 : 4 : 0.8
     No reaction could have occurred since diffusion measurement was taken within 0.5-1.0 hour after mixing.

7. ^{29}Si NMR spectra (ref. TMS) for TEOS reaction mixture.
   molar ratio for this and the following systems, unless stated otherwise, is
   TEOS : EtOH : H_2O : HCl = 1 : 4 : 0.8 : 0.0008

8. Peak assignments of ^{29}Si NMR multiplets due to different environment of adjacent silicon. Symbols follow those of Kelts and Armstrong [24], where square and circle represents resonating and adjacent silicon, respectively.

9. Time evolution of silicon species as detected by ^{29}Si NMR.

10. Gas chromatograms for TEOS reaction mixtures.

11. Molecular size distribution of silicon oligomers as determined by GC-FID.

12. Hydrolysis and condensation of TEOS: water and ethanol content, calculated from ^{29}Si NMR results.

13. ^{29}Si NMR spectrum for system:
molar ratio TEOS : EtOH : H_2O : HCl = 1 : 4 : 0.5 : 0.0005
reaction time 1 month.

14. Mobility of silicon oligomers as affected by the extent of hydrolysis.
Hydrolysis initiated by addition of water to a 3-month-old sample with the same molar composition as in (13), making the total water-to-silicon ratio, W/Si, to be 0.8 and 1.0.

15. Diffusion coefficients of silicon oligomers

* from extrapolation

Figure 1

-OH from water,
ethanol and silanol
(fast chemical exchange)

-SiO-CH₂-

HO-CH₂-

-SiO-CH₂CH₃

HO-CH₂CH₃
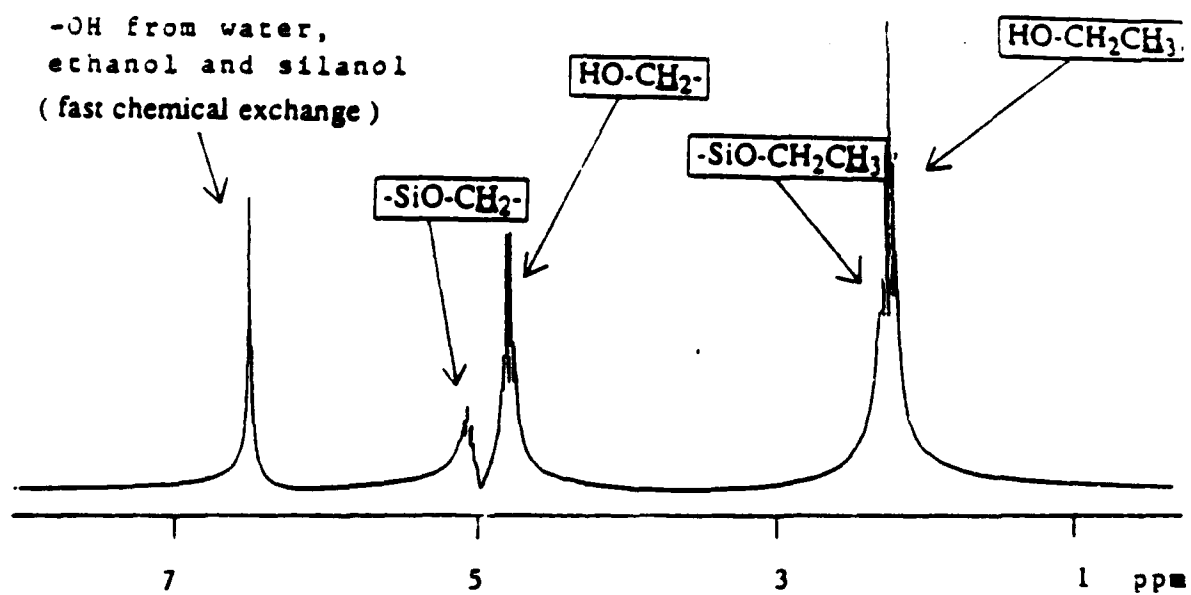
Figure 2

Figure 3

Figure 4

-OH from water,
ethanol and silanol

(fast chemical exchange)

HO-CH₂-

HO-CH₂CH₃

7   5   3   ppm
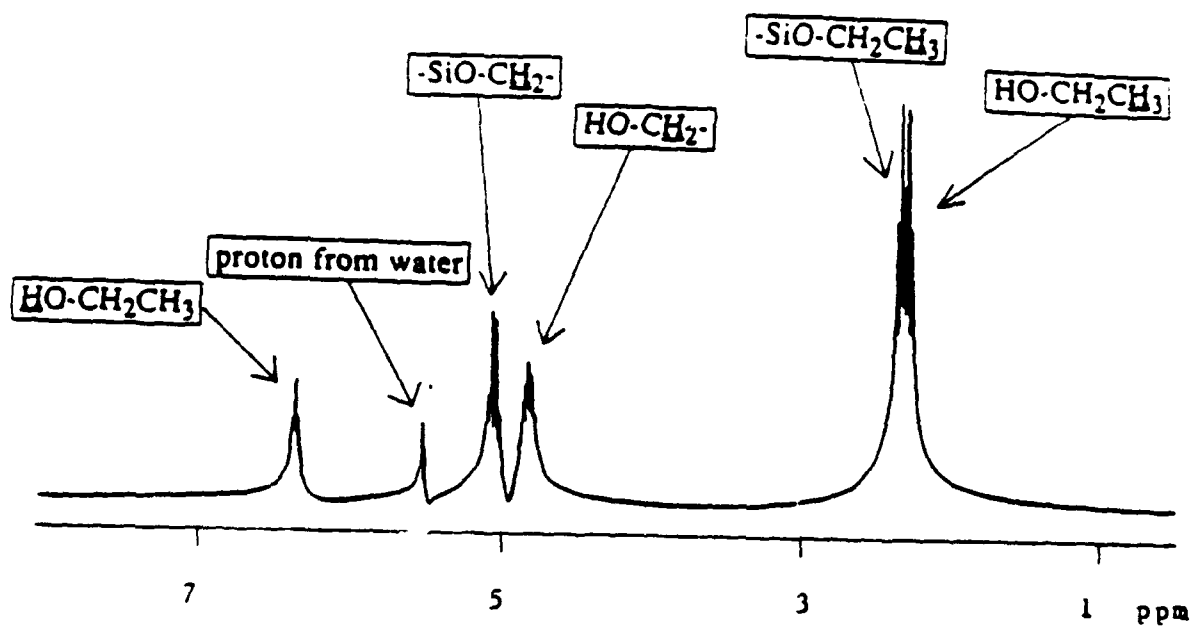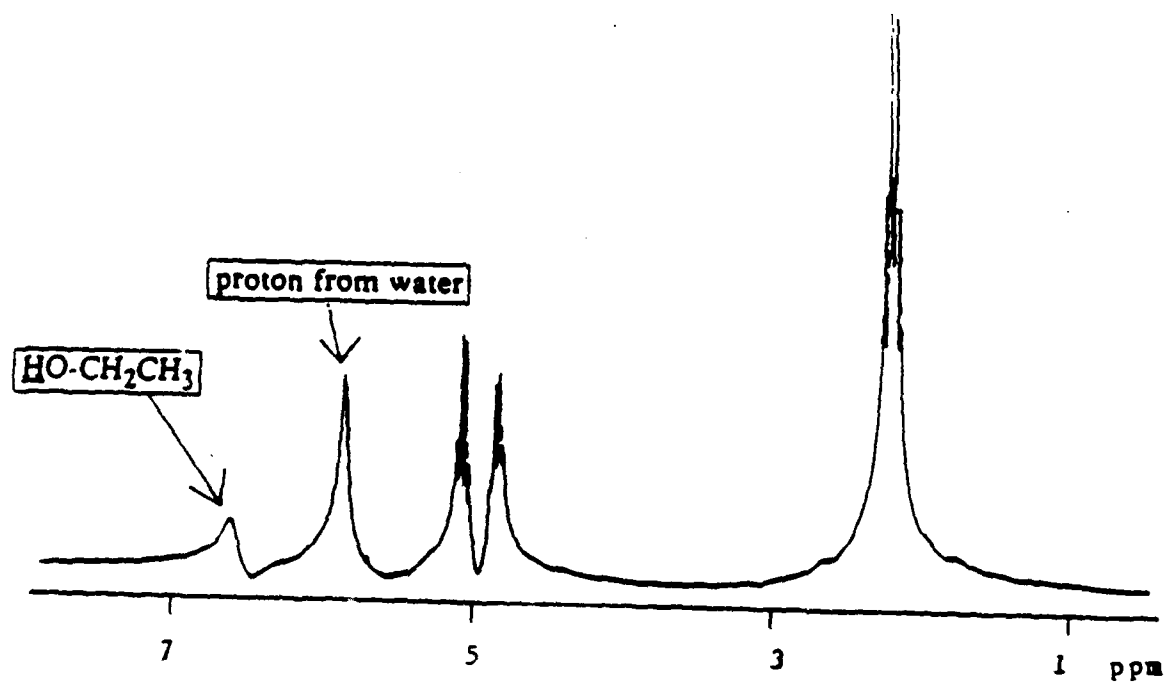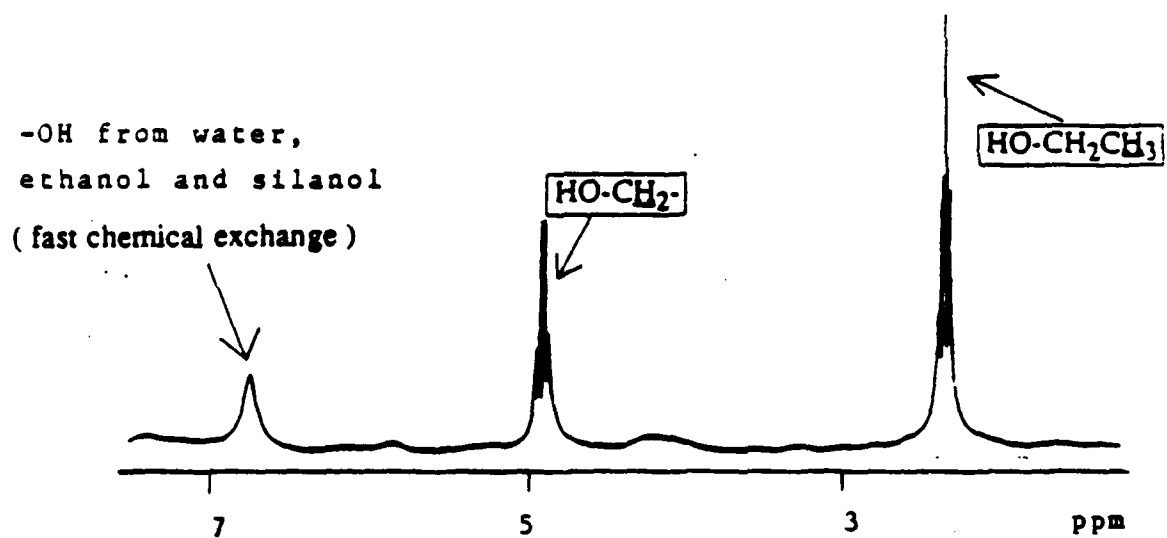
Figure 5

(a) Time = 25 h
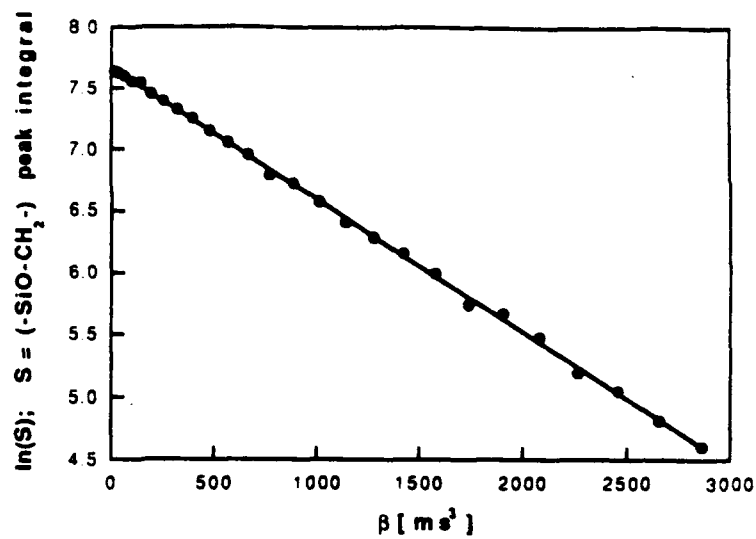
(b) Time = 128 h
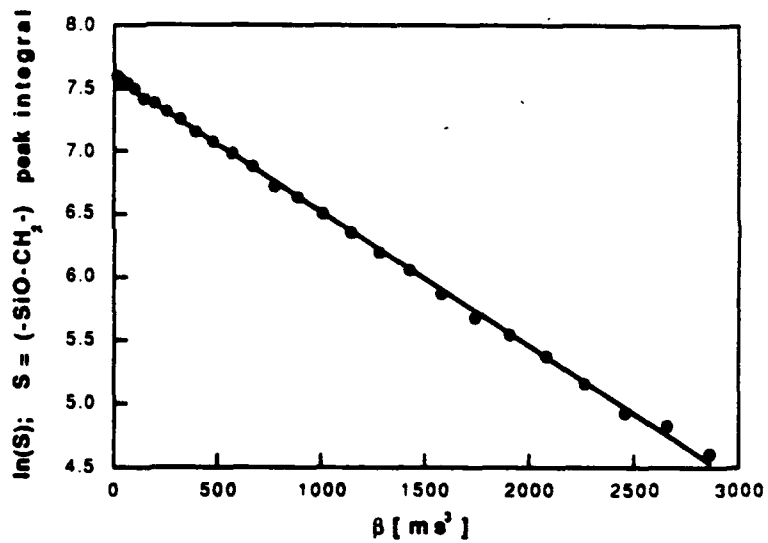
(c) Time = 466 h

Figure 6

Figure 7

(a) 15 h

(b) 51 h

(c) 73 h

(d) 90 h

OH

Si-O-Si-(OEt)$_2$

Si-O-Si-(OEt)$_3$

TEOS

(HO)-Si-(OEt)$_3$

(SiO)$_2$-Si-(OEt)$_2$

cyclic
tetramer

linear

-80   -84   -38   -92   -96   ppm

Figure 7

(e) 113 h

(SiO)-Si-(OEt)₃

(SiO)-Si-(OH)(OEt)₂

TEOS

(f) 152 h

(SiO)₂-Si-(OEt)₂

cyclic
tetramer   linear

(g) 178 h

(h) 456 h

-80   -84   -88   -92   -96   ppm
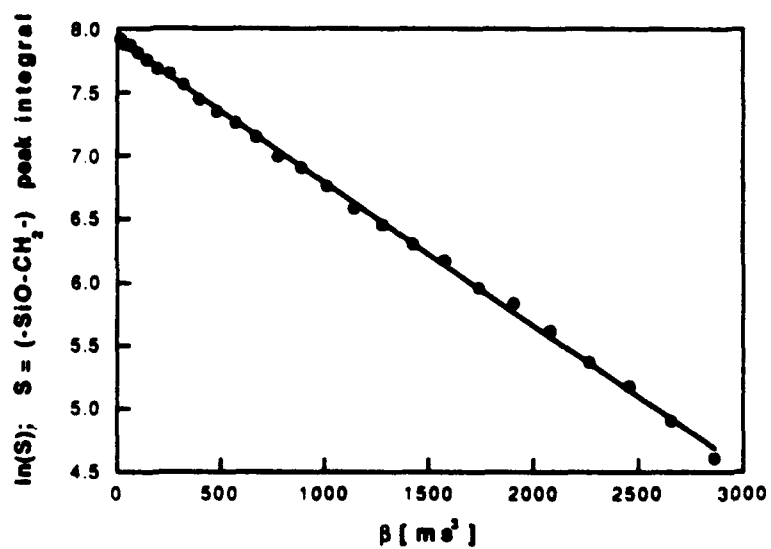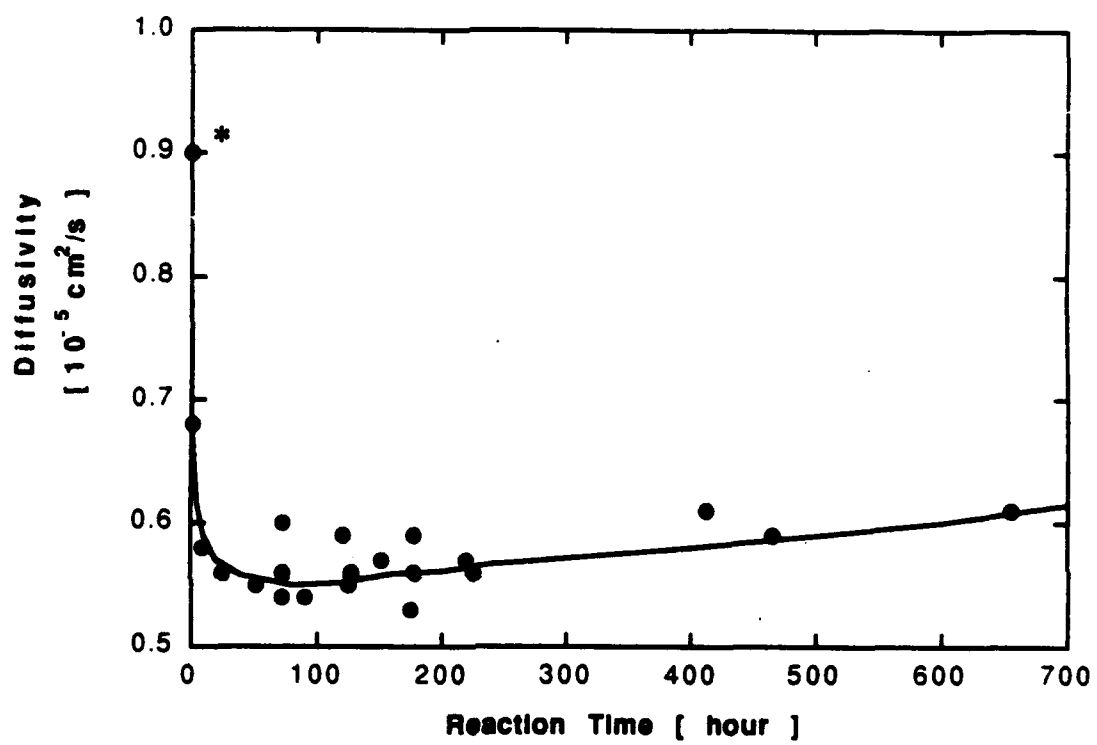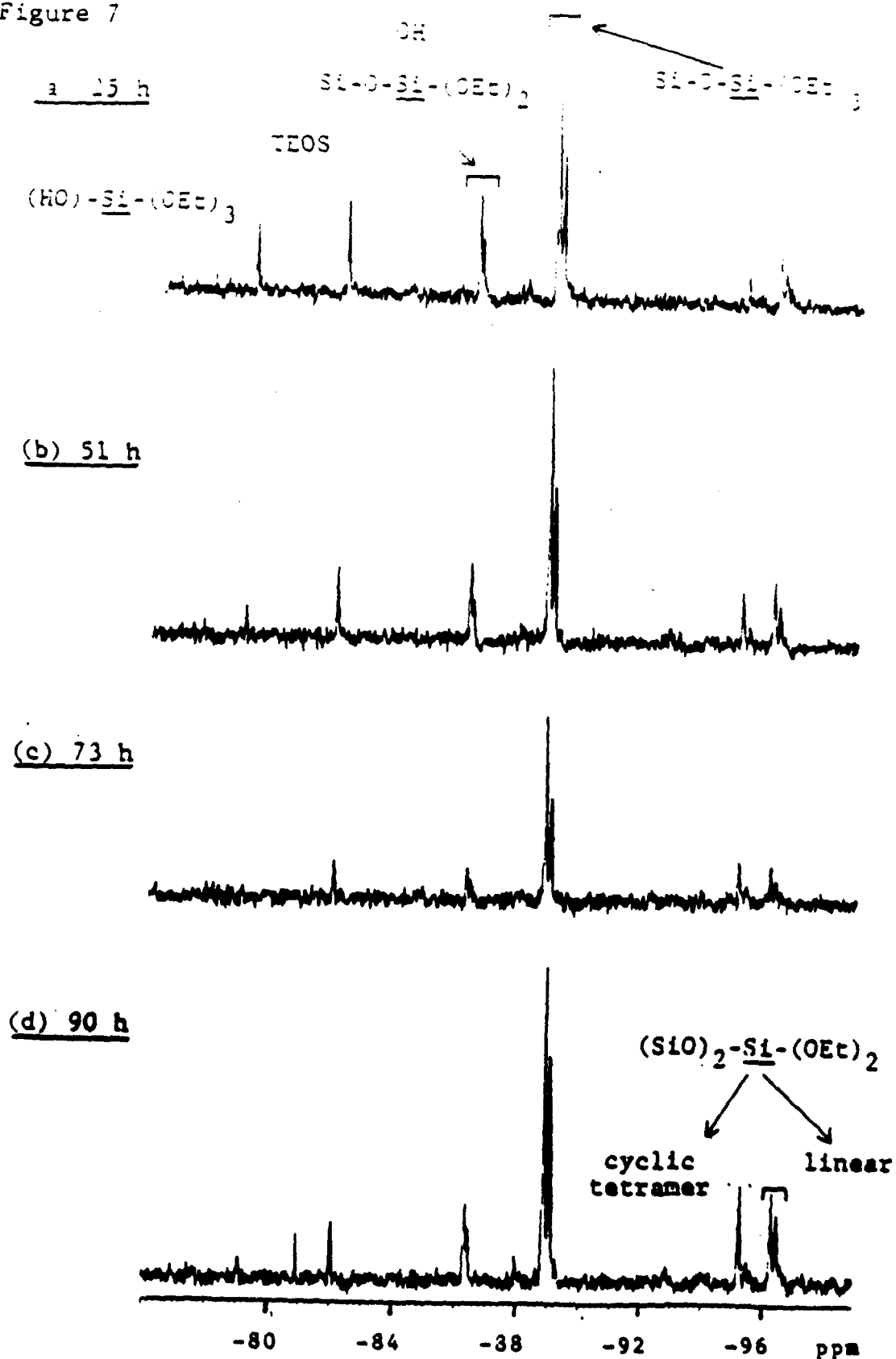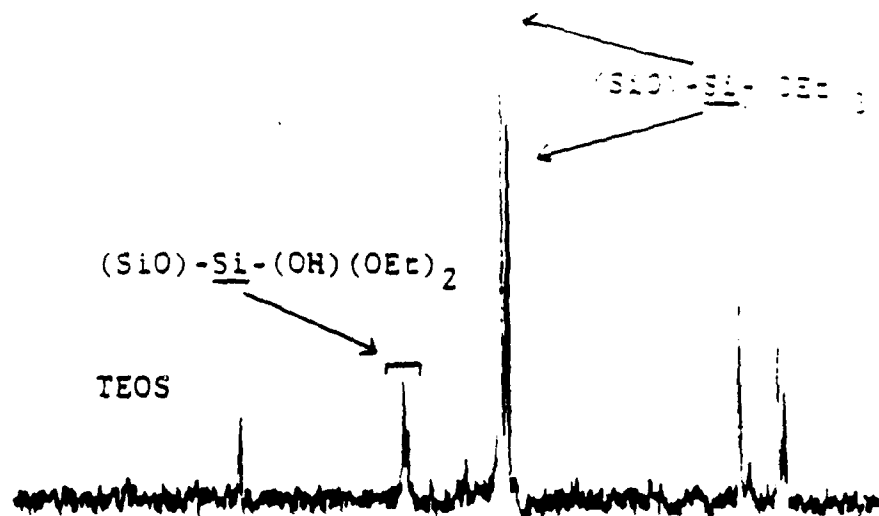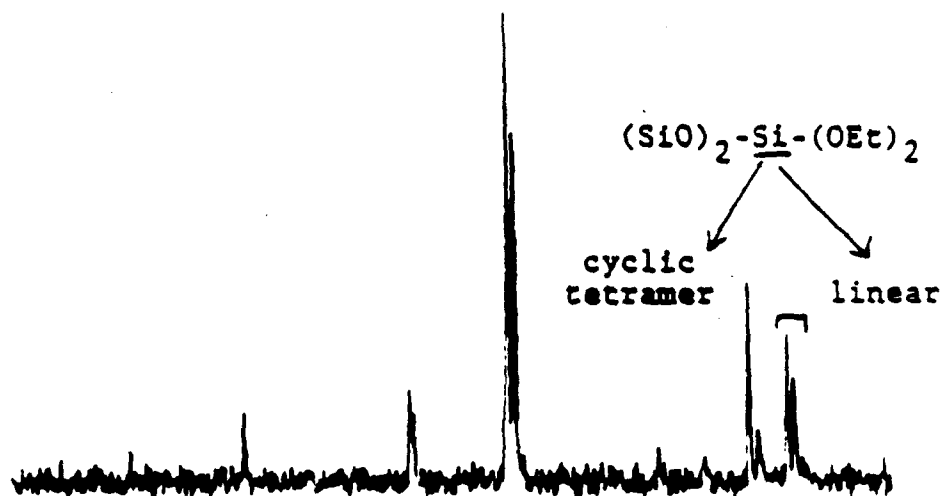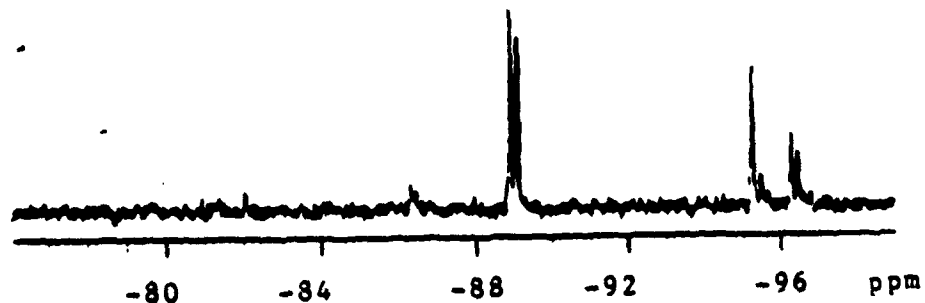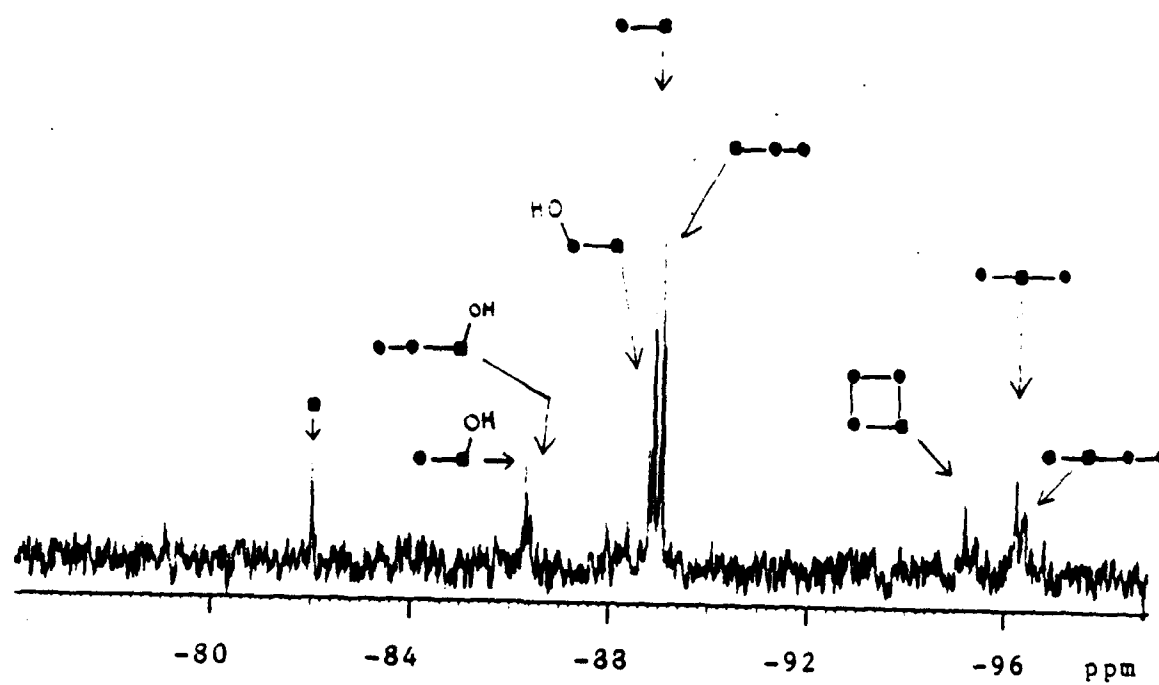
Figure 8

Figure 9

(a)   unsubstituted silicon
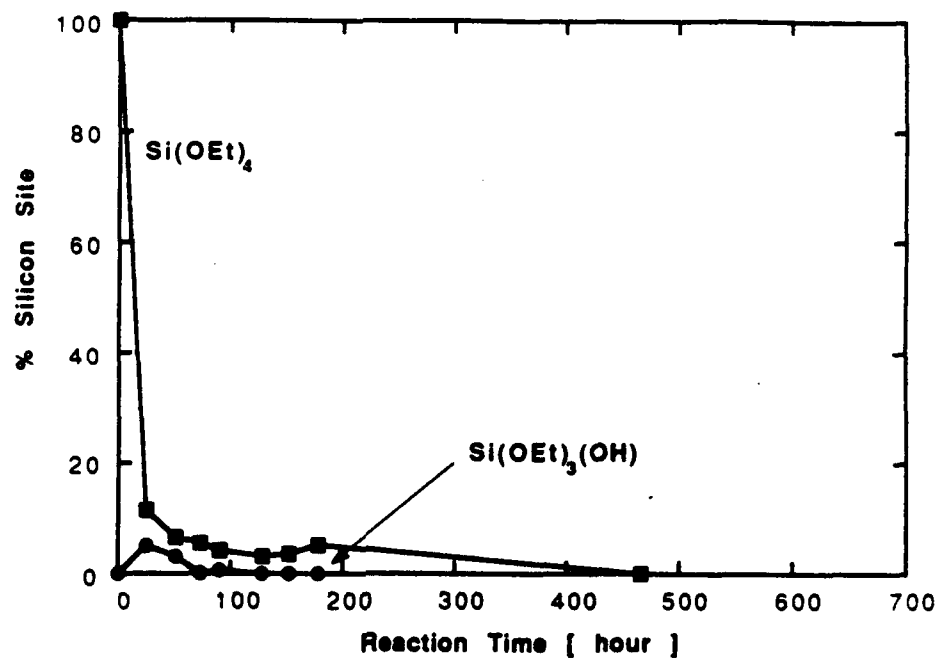
(b)   monosubstituted silicon
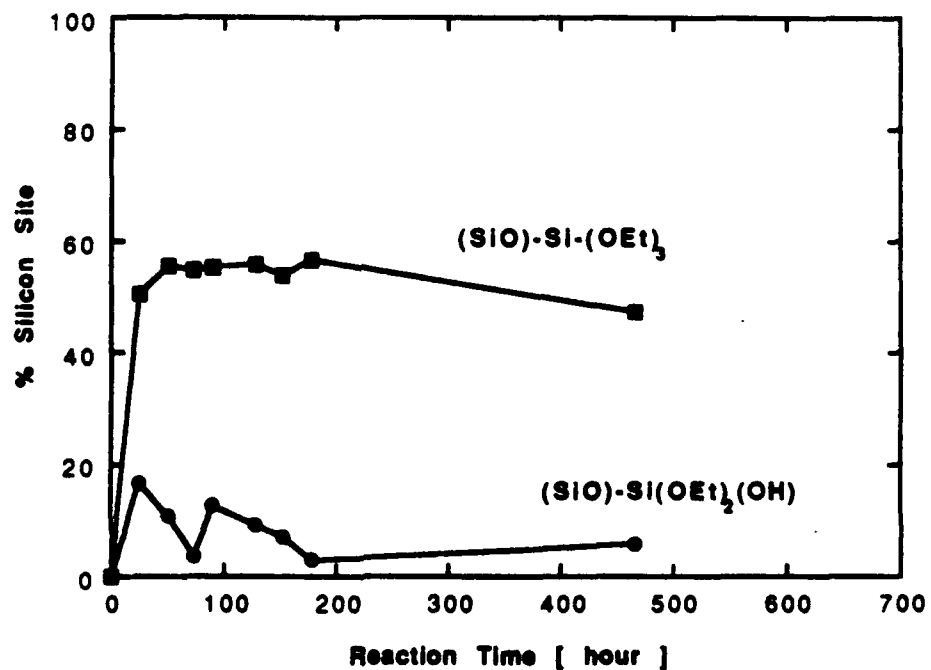
Figure 9

(c)   disubstituted   silicon

$(SiO)_2$-Si-$(OEt)_2$ (cyclic tetramer)

$(SiO)_2$-Si-$(OEt)_2$ (linear)

Figure 10

0.25 h

1.25 h

2.25 h

4.28 h

monomers

dimers

trimers

0   12   24
Retention Time (min)
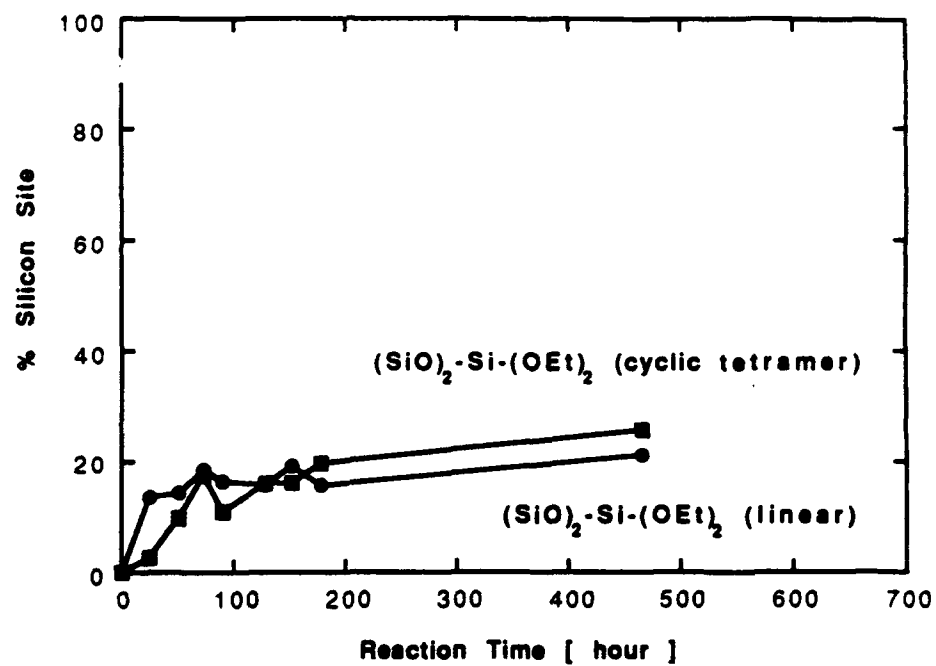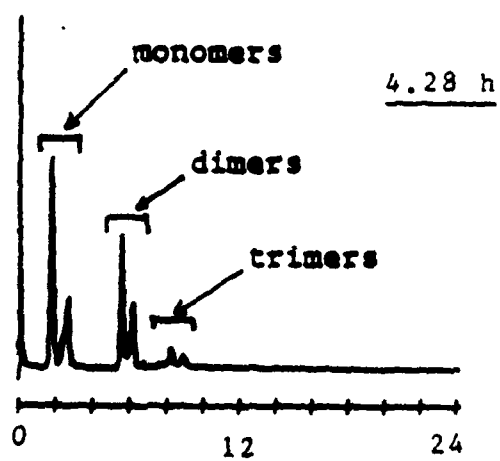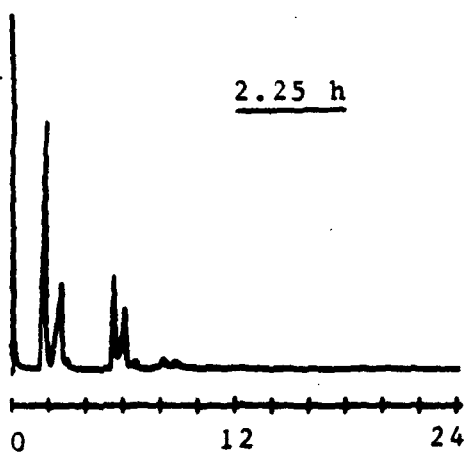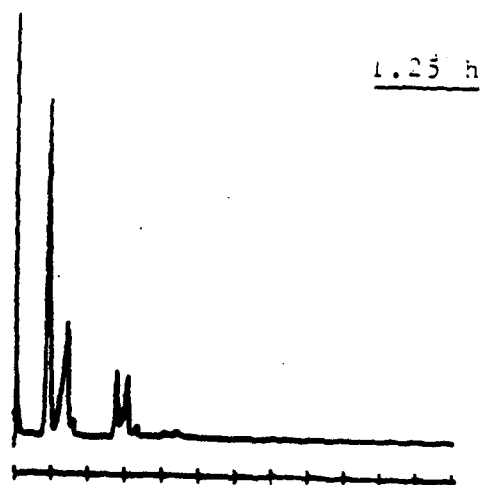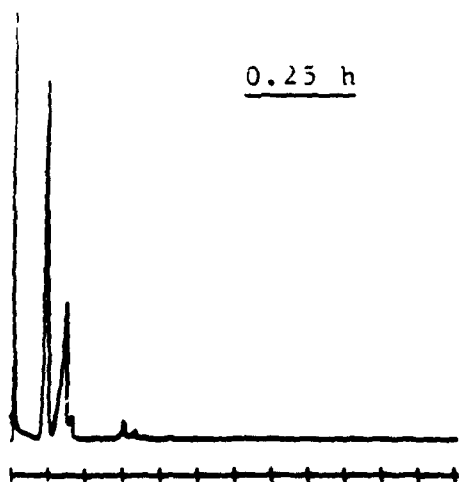
0   12   24
Retention Time (min)

Figure 10
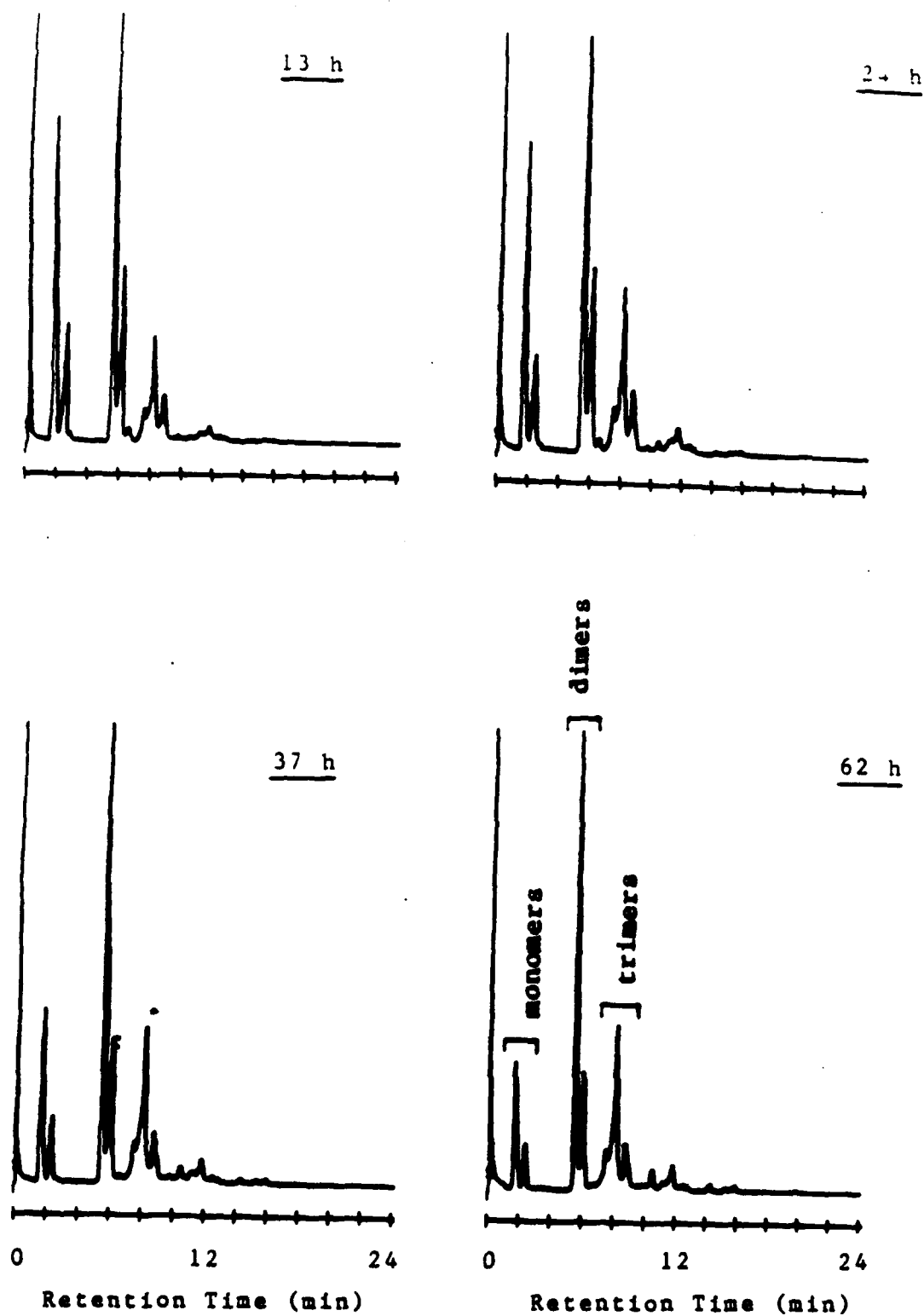
Figure 10
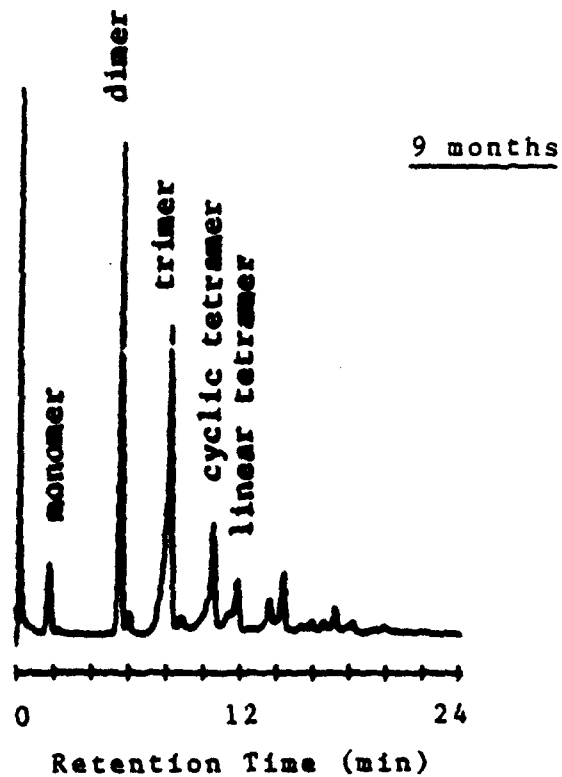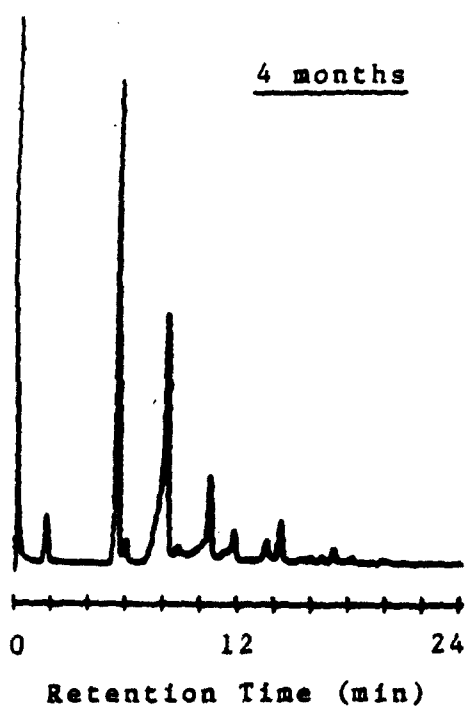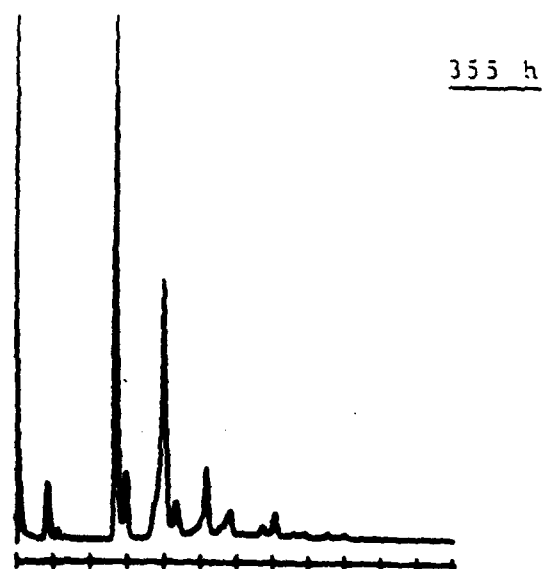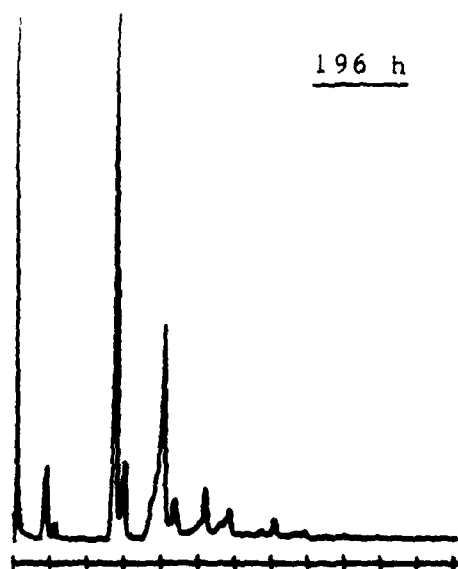
Figure 11

(a) monomeric species
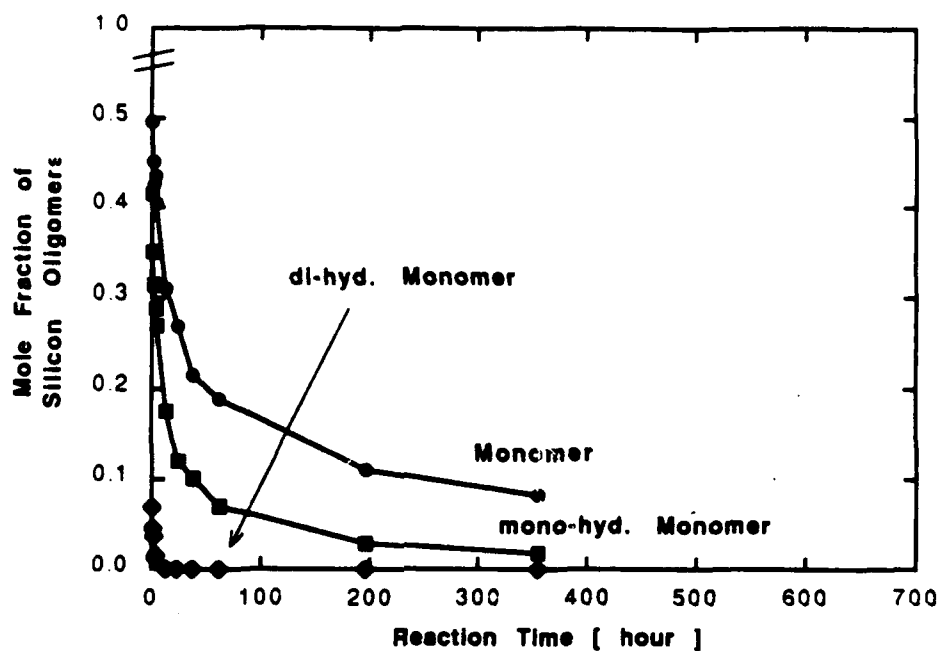
(b) dimeric species
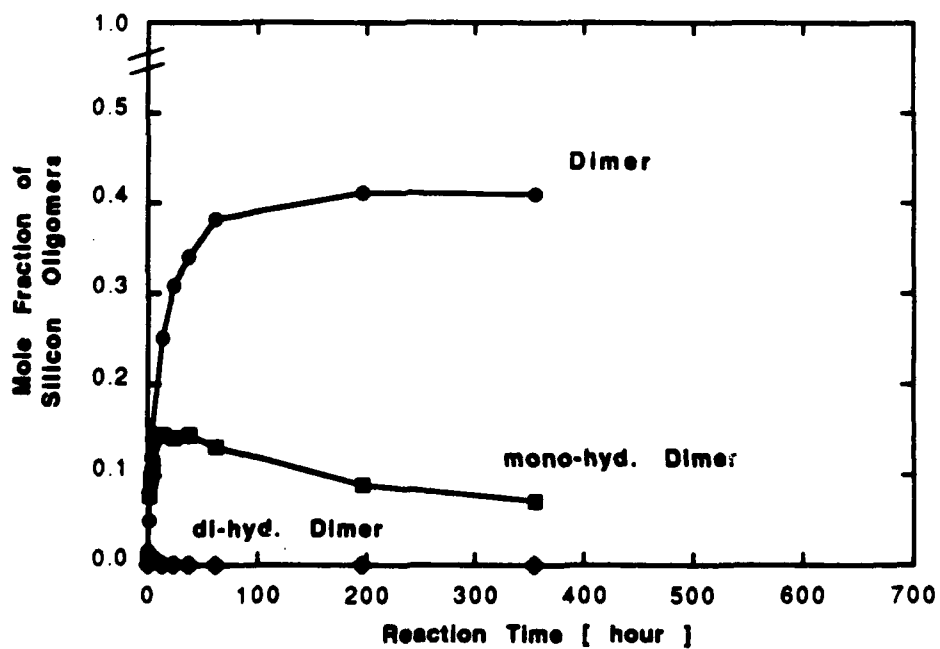
Figure 11

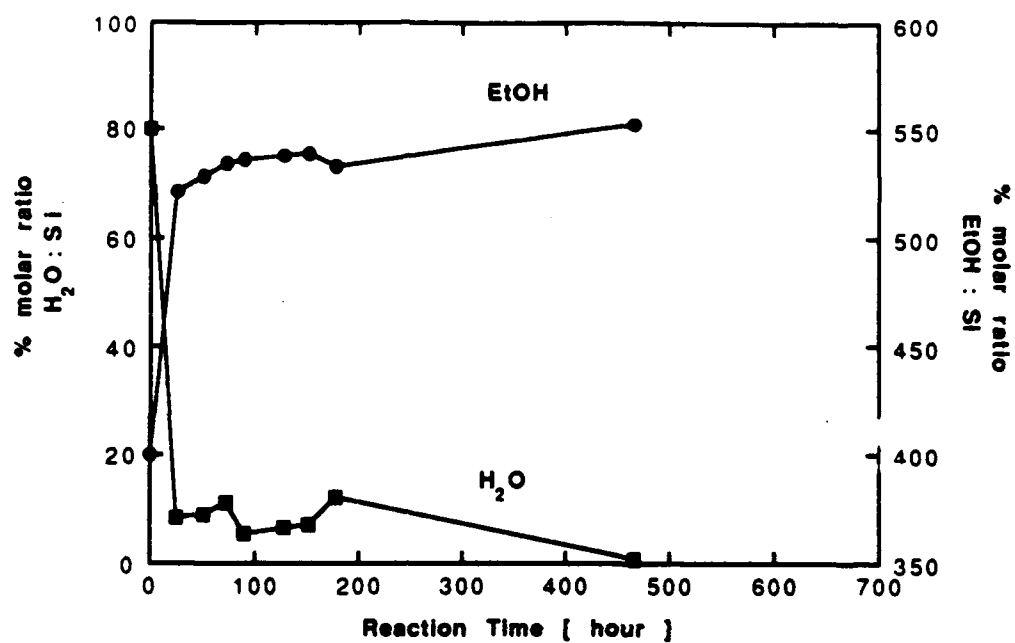(c)   trimeric species
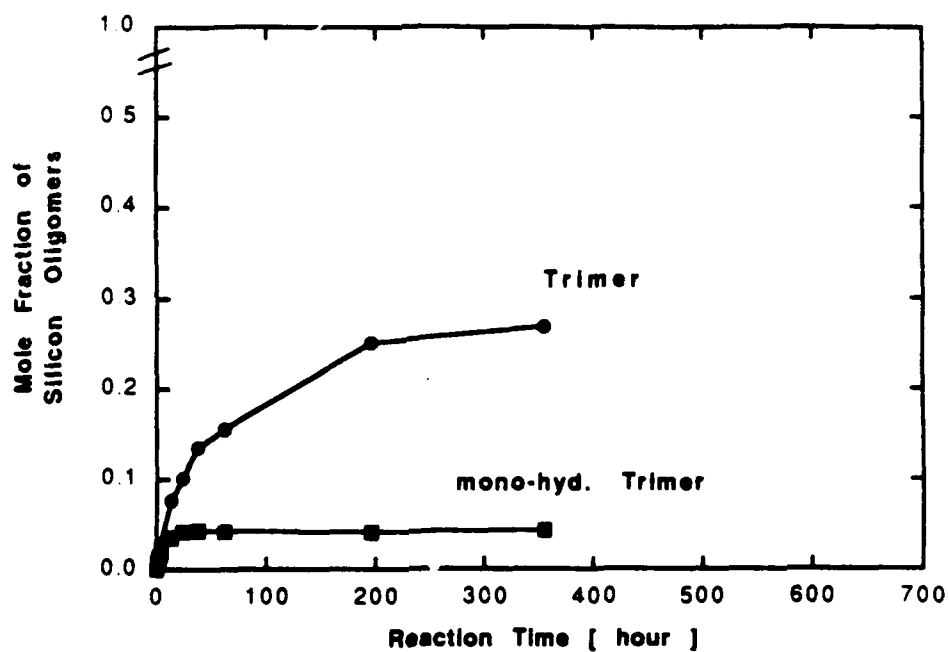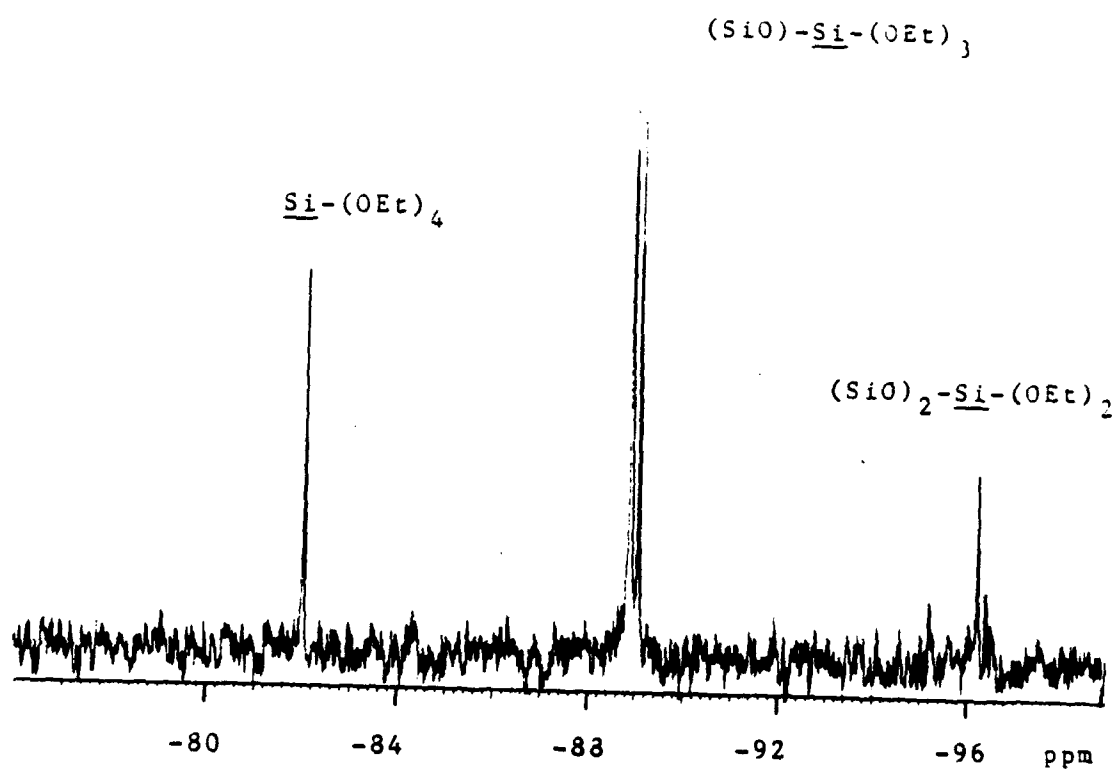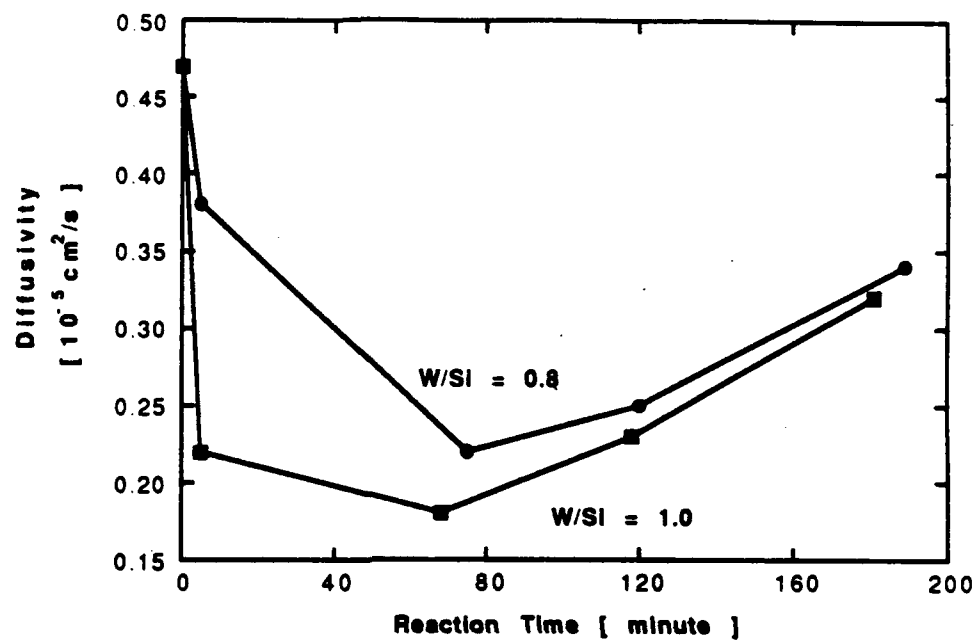

(d)   tetrameric species

Figure 12

Figure 13

$\underline{Si}-(OEt)_4$

$(SiO)-\underline{Si}-(OEt)_3$

$(SiO)_2-\underline{Si}-(OEt)_2$

-80   -84   -88   -92   -96   ppm
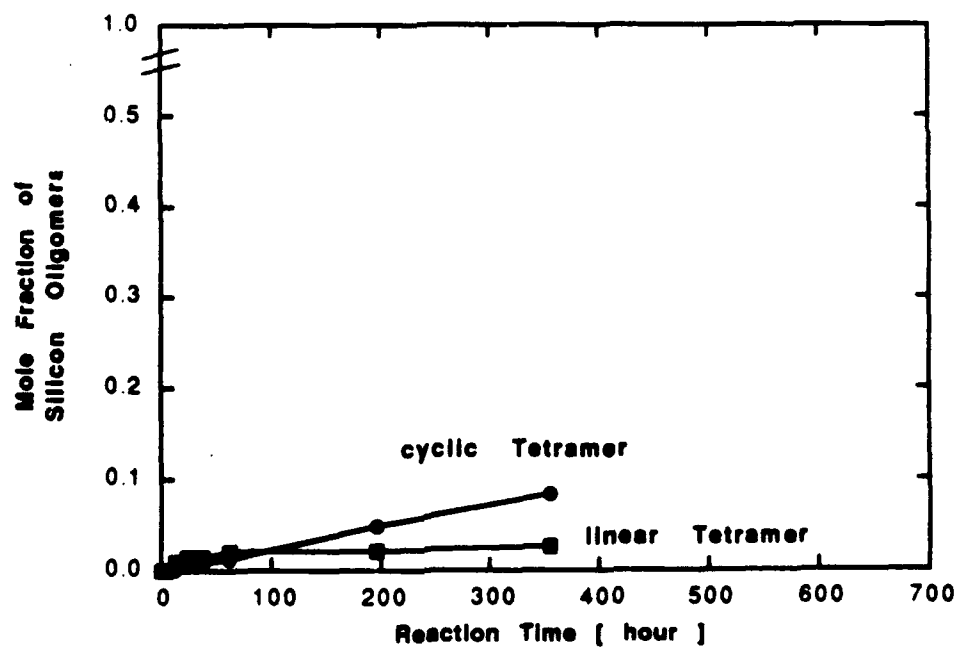
Figure 14

(a)   average diffusivity

(b)   extent of hydrolysis

Figure 15